Syntheses, Structures, and DFT Calculations of Phosphenium Phosphite Complexes of Molybdenum: Preference of Nonbridging Form to Bridging Form of a Donor Group

Hiroshi Nakazawa,*[,§] Yasutaka Miyoshi,[†] Takafumi Katayama,[†] Tsutomu Mizuta,[†] Katsuhiko Miyoshi,[†] Noriko Tsuchida,[‡] Ayako Ono,[‡] and Keiko Takano[‡]

Department of Chemistry, Graduate School of Science, Osaka City University, Sumiyoshi-ku, Osaka 558-8585, Japan, Department of Chemistry, Graduate School of Science, Hiroshima University, Higashi-Hiroshima 739-8526, Japan, and School of Integrated Sciences, Graduate School of Humanities and Sciences, Ochanomizu University, Bunkyo-ku, Tokyo 112-8610, Japan

Received July 14, 2006

Molybdenum carbonyl complexes with two and three diamino-substituted phosphites, *cis*-[$Mo(CO)_4${$P(NMeCH_2)_2(OMe)$}$_2$] (**1a**) and *fac*-[$Mo(CO)_3${$P(NMeCH_2)_2(OMe)$}$_3$] (**2a**), react with TMSOTf to give the corresponding cationic phosphenium phosphite complexes, *cis*-[$Mo(CO)_4${$P(NMeCH_2)_2(OMe)$}{$P(NMeCH_2)_2$}](OTf) (**1b**) and *fac*-[$Mo(CO)_3${$P(NMeCH_2)_2(OMe)$}$_2${$P(NMeCH_2)_2$}](OTf) (**2b**), respectively, by single OMe^- abstraction from the coordinating phosphite. The X-ray structure analyses and the NMR spectra of the products showed that the original configuration around the Mo is retained with the OMe group(s) on the remaining phosphite ligand(s) free from the interaction with the phosphenium phosphorus. A related phosphite complex, CpMo(CO)(I){$P(NMeCH_2)_2(OMe)$}$_2$ (**3**), was converted in the reaction with $NaK_{2.8}$ into a neutral phosphenium complex, CpMo(CO){$P(NMeCH_2)_2(OMe)$}{$P(NMeCH_2)_2$} (**4**), in which no such significant MeO···P (phosphenium) bridging interaction was also observed. DFT calculations have been incorporated to study the preference of the nonbridging form for phosphenium phosphite complexes, together with the preference of the bridging form for the analogous silylene alkoxysilyl complexes, and revealed that the bridging requires larger geometrical changes for phosphenium phosphite complexes than for silylene alkoxysilyl complexes.

Introduction

The wide-ranging applications of metal carbenes (M═C) in organometallic chemistry have aroused interest in transition metal complexes containing metal−heteroatom multiple bonds.[1] A cationic phosphenium ($^+PR_2$) has attracted significant attention as a ligand for transition metals, knowledge on cationic phosphenium complexes has been accumulated, and some review articles appeared recently.[2−6] Phosphenium is isolobal with a singlet carbene and its heavier congeners in terms of possessing the lone pair electrons, the vacant p orbital, and two substituents on the central atom. The comparison of phosphenium complexes with silylene complexes is particularly interesting because both P and Si are situated in the same third row of the periodic table. Both phosphenium and silylene ligands show electrophilicity, and two structures, i.e., nonbridging and bridging forms, are conceivable for a *cis* phosphenium phosphite complex and a *cis* silylene alkoxysilyl complex (Figure 1). However, their preferential structure is subtly dependent on the heteroatom involved.

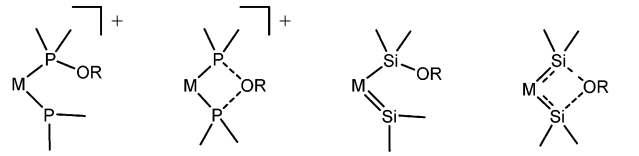

Figure 1. (1) Phosphenium phosphite complex and (2) silylene silyl complex.

Some cationic complexes with both phosphenium and phosphite ligands in a *cis* position have been reported, which are shown in Figure 2.[7] Their NMR data suggest exclusive formation of nonbridging complexes. In contrast, all the complexes reported to date, which have both a silylene ligand and an alkoxysilyl ligand (or a related silyl ligand) in a *cis* position, adopt bridging forms, as shown in Figure 3.[8]

* Corresponding author. Fax: +81-6-6605-2522. Tel: +81-6-6605-2547. E-mail: nakazawa@sci.osaka-cu.ac.jp.
§ Osaka City University.
† Hiroshima University.
‡ Ochanomizu University.

(1) Nugent, W. A.; Mayer, J. M. In *Metal-Ligand Multiple Bonds*; Wiley: New York, 1988.
(2) Cowley, A. H.; Kemp, R. A. *Chem. Rev.* **1985**, *85*, 367.
(3) (a) Sanchez, M.; Mazieres, M. R.; Lamande, L.; Wolf, R. In *Multiple Bonds and Low Coordination in Phosphorus Chemistry*; Regitz, M., Scherer, O. J., Eds.; Thieme: New York, 1990; Chapter D1. (b) Schmidpeter, A. In *Multiple Bonds and Low Coordination in Phosphorus Chemistry*; Regitz, M., Scherer, O. J., Eds.; Thieme: New York, 1990; Chapter D2.
(4) Gudat, D. *Coord. Chem. Rev.* **1997**, *163*, 71.
(5) Nakazawa, H. *J. Organomet. Chem.* **2000**, *611*, 349.
(6) Nakazawa, H. *Avd. Organomet. Chem.* **2004**, *50*, 107.
(7) (a) Nakazawa, H.; Yamaguchi, Y.; Mizuta, T.; Miyoshi, K. *Organometallics* **1995**, *14*, 4173. (b) Nakazawa, H.; Yamaguchi, T.; Miyoshi, K.; Nagasawa, A. *Organoemtallics* **1996**, *15*, 2517. (c) Yamaguchi, Y.; Nakazawa, H.; Kishishita, M.; Miyoshi, K. *Organometallics* **1996**, *15*, 4383.
(8) (a) Okazaki, M.: Tobita, H.; Ogino, H. *J. Chem. Soc., Dalton Trans.* **2003**, 493, and references therein. (b) Okazaki, M.; Minglana, J. J. G.; Yamahira, N.; Tobita, H.; Ogino, H. *Can. J. Chem.* **2003**, *81*, 1350. (c) Goikhman, R.; Karakuz, T.; Shimon, L. J. W.; Leitus, G.; Milstein, D. *Can. J. Chem.* **2003**, *83*, 786. (d) Koshikawa, H.; Okazaki, M.; Matsumoto, S.; Ueno, K.; Tobita, H.; Ogino, H. *Chem. Lett.* **2005**, *34*, 1412.

10.1021/om060639x CCC: $33.50
Publication on Web 11/09/2006

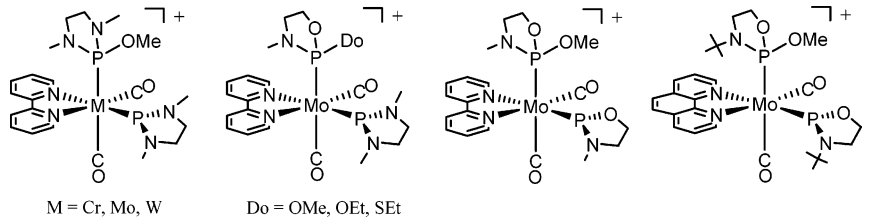

Figure 2. Cationic *cis* complexes with phosphenium and phosphite ligands. All of them adopt nonbridging forms.

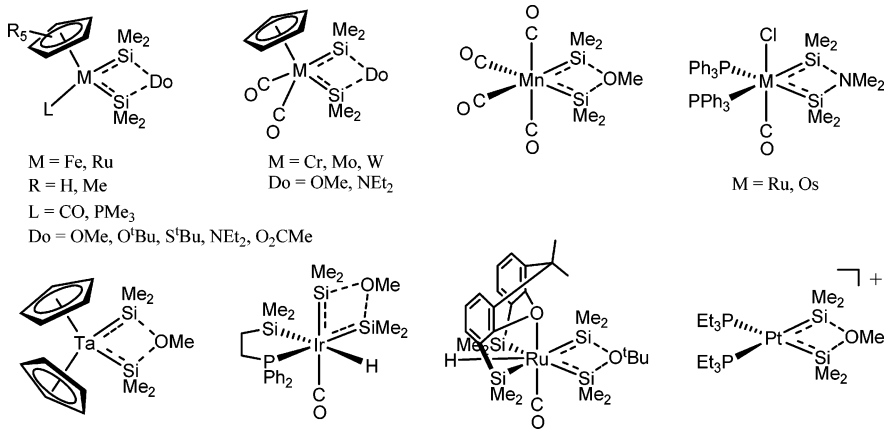

Figure 3. *Cis* complexes with silylene and alkoxysilyl (or a related silyl) ligands. All of them adopt bridging forms.

It should be noted that all silylene silyl complexes in Figure 3 except the Ir complex have a mirror plane containing the bridging donor group, whereas phosphenium phosphite complexes cannot have a mirror symmetry even if it takes a bridging form. To elucidate whether the asymmetric molecular structure is the reason for phosphenium phosphite complexes taking a nonbridging structure exclusively, we prepared phosphenium phosphite complexes that possess a mirror plane in the bridging form. In this paper, we report the preparation of *cis*-$Mo(CO)_4$-$\{P(NMeCH_2)_2(OMe)\}_2$ (**1a**), *fac*-$Mo(CO)_3\{P(NMeCH_2)_2(OMe)\}_3$ (**2a**), and $CpMo(CO)I\{P(NMeCH_2)_2(OMe)\}_2$ (**3**) and their reactions with TMSOTf or $NaK_{2.8}$ to give the corresponding phosphenium phosphite complexes. The X-ray structures of the products and density functional theory (DFT) calculations have also been reported.

Results and Discussion

Complexes bearing both phosphenium and phosphite ligands have been obtained by the reaction of a monophosphite complex with a Lewis acid to give a phosphenium complex, followed by CO/phosphite substitution reaction.[7a] A typical reaction sequence is shown in eq 1.

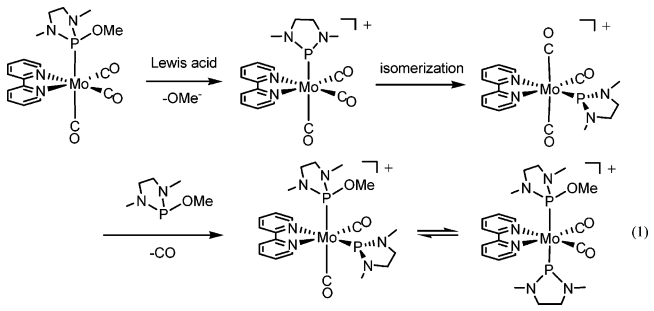

The stability of cationic phosphenium complexes increases with the number of amino substituents on the phosphenium phosphorus. Since a phosphenium ligand is a strong π-accepting ligand, electron-donating bpy is favorable as an ancillary ligand rather than CO. However, the bpy−CO mixed ligand system causes complicated stereochemistry around a central metal in phosphenium phosphite complexes. Therefore, we chose *cis*-$Mo(CO)_4L_2$ and *fac*-$Mo(CO)_3L_3$, where L stands for $P(NMeCH_2)_2(OMe)$, as a starting complex. $CpMo(CO)IL_2$ was also selected in the hopes of preparing $CpMo(CO)L\{P(NMeCH_2)_2\}$ in the reaction with $NaK_{2.8}$ and then TMSOTf.

Synthesis of *cis*-$Mo(CO)_4L_2$ (1a), *fac*-$Mo(CO)_3L_3$ (2a), and $CpMo(CO)IL_2$ (3). Complex **1a** was obtained from $Mo(CO)_4$(nbd) (nbd = 2,5-norbornadiene) and 2 equiv of L in 83% yield. The reaction of $Mo(CO)_4(piperidine)_2$ with L also yielded **1a**, but $Mo(CO)_3L_3$ was a contaminant and its elimination was difficult. Complex **2a** was prepared from $Mo(CO)_3(NCMe)_3$ and 3 equiv of L in 71% yield. Complex **3** was prepared in the photoreaction of $CpMo(CO)_3I$ with 2 equiv of L in 81% yield. These complexes were fully characterized by ^1H, ^{13}C, and ^{31}P NMR and IR spectra and elemental analyses. Some resonances in the ^1H NMR spectra were observed as a filled-in doublet (fd).[9] Complex **2a** was characterized by X-ray analysis.

Reaction of 1a and 2a with TMSOTf. Treatment of **1a** with an equimolar amount of TMSOTf yielded *cis*-$[Mo(CO)_4\{P(NMeCH_2)_2(OMe)\}\{P(NMeCH_2)_2\}]OTf$ (**1b**) (eq 2). Although the reaction is very clean and the product **1b** is stable in solution unless exposed to air, the stability of **1b** in the solid state is not enough to obtain sufficient elemental analysis data. The reaction of **1a** with excess TMSOTf did not yield a diphosphenium complex. The ^{31}P NMR spectrum of **1b** showed two broad resonances at about 285 and 140 ppm at room temperature, but the spectrum at −60 °C exhibited two doublets at 285.01 and 139.42 ppm with J_{PP} = 42.5 Hz due to phosphenium and phosphite ligands, respectively. This shows that **1b** is a phosphenium phosphite complex with a nonbridging form. The value of the coupling constant indicates a *cis* configuration. The broadening at room temperature may be the

(9) Redfield, D. A.; Cary, L. W.; Nelson, J. H. *Inorg. Chem.* **1975**, *14*, 50.

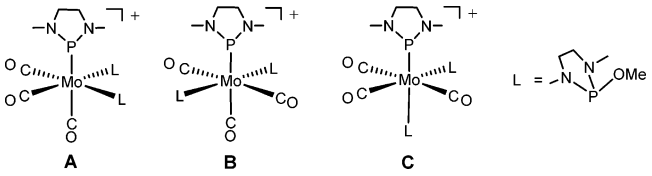

Figure 4. Three possible structures for $[Mo(CO)_3L_2\{P(NMeCH_2)_2\}]^+$.

symptom of slow OMe group migration from the phosphite P to the phosphenium P. The X-ray structure analysis confirmed the phosphenium phosphite complex with a *cis* configuration (vide infra). This is the first phosphenium phosphite complex with CO ancillary ligands only.

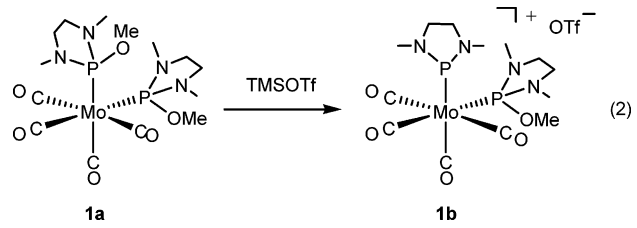

(2)

Reaction of **2a** with equimolar amount of TMSOTf generated *fac*-$[Mo(CO)_3\{P(NMeCH_2)_2(OMe)\}_2\{P(NMeCH_2)_2\}]OTf$ (**2b**) (eq 3). The phosphenium complex is also too reactive in the solid state to obtain sufficient elemental analysis data. The reaction of **2a** with excess TMSOTf generated neither a diphosphenium complex nor a triphosphenium complex, but rather a monophosphenium complex, **2b**. The ^{31}P NMR spectrum of **2b** showed broad resonances at room temperature presumably due to slow OMe migration, but the spectrum at −60 °C exhibited a triplet at 275.74 ppm and a doublet at 141.84 ppm with $J_{PP} = 41.7$ Hz. The triplet is attributable to a phosphenium P, and the doublet is due to two phosphite P's. There are three possible structures (**A**−**C**) for a monophosphenium diphosphite complex (Figure 4). Since **C** has two magnetically different phosphites, the possibility of **C** can be ruled out. **A** and **B** may be distinguished from the ^{13}C NMR spectrum in the CO region. However, the spectrum showed a multiplet at about 210 ppm. Thus it could not identify the geometrical structure. The X-ray structure analysis of **2b** revealed that the isolated complex has a type **A** structure with a nonbridging OMe group on the phosphite ligand (vide infra).

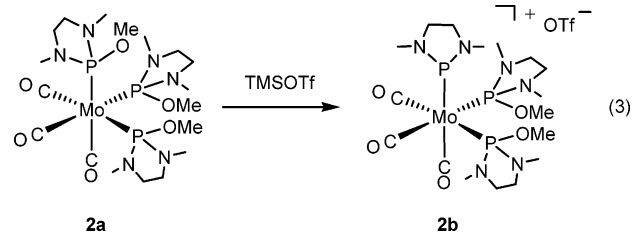

(3)

Reaction of 3 with $NaK_{2.8}$. We expected the formation of $CpMo(CO)\{P(NMeCH_2)_2(OMe)\}\{P(NMeCH_2)_2\}$ (**4**) in the following two-step reaction: reduction of **3** with $NaK_{2.8}$ to produce an anionic complex, $[CpMo(CO)\{P\{NMeCH_2\}_2(OMe)\}_2]^-$, and OMe^- abstraction with TMSOTf to give $[CpMo(CO)\{P\{NMeCH_2\}_2(OMe)\}\{P\{NMeCH_2\}_2\}]$ (**4**). The desired product **4** was obtained unexpectedly in the reaction of **3** with $NaK_{2.8}$ (eq 4). The ^{31}P NMR spectrum exhibited two doublets at 250.44 and 194.74 ppm with $J_{PP} = 61.2$ Hz, showing that **4** takes a nonbridging form. The X-ray structure analysis confirmed the nonbridging structure (vide infra).

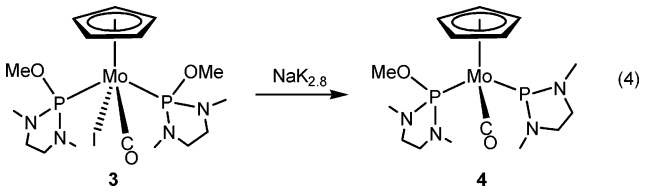

(4)

X-ray Structures of 1b, 2a, 2b, and 4. The X-ray crystal structures of cationic phosphenium complexes **1b** and **2b** and that of neutral phosphenium complex **4** were determined. The X-ray structure of the corresponding phosphite complex **2a** was also determined for comparison. Their ORTEP drawings are given in Figures 5−8. The crystallographic data and selected bond distances and angles are summarized in Tables 1 and 2.

Complexes **1b**, **2a**, and **2b** have octahedral configurations with a *cis* geometry for **1b** and *fac* geometries for **2a** and **2b**, as expected from their NMR data. Complex **4** has a typical piano-stool configuration. Bond distances of Mo(1)−P(1) in **1b**, Mo(1)−P(1), Mo(1)−P(2), and Mo(1)−P(3) in **2a**, and Mo(1)−P(1) and Mo(1)−P(2) in **2b** fall in the range of normal Mo−P dative bond distances (2.40−2.57 Å).[2] In contrast, the Mo(1)−P(2) (2.3178(6) Å) bond in **1b** and the Mo(1)−P(3) (2.3145(10) Å) bond in **2b** are clearly shorter than the normal Mo−P dative bond. The sum of the angles around P2 in **1b** and that around P3 in **2b** are 359.51° and 358.93°, respectively, showing that these phosphenium P's have planar geometries. These data suggest that Mo−P(phosphenium) has considerable double-bond character, which may be caused by back-donation from Mo to phosphenium P. These phosphenium P's get some electron density from their amino substituent(s) in addition to the Mo fragment, because P(phosphenium)−N bonds are shorter than P(phosphite)−N bonds: 1.613(2) and 1.617(2) Å versus 1.661(2) and 1.652(2) Å for **1b**, 1.620(4) and 1.624(4) Å versus 1.670(4), 1.670(4), 1.654(4), and 1.679(4) Å for **2b**. The electron donation from amino substituents to phosphenium P is not observed for *trans*-$[Mo(bpy)(CO)_2\{P(NMeCH_2)_2(OMe)\}\{P(NMeCH_2)_2\}](OTf)$ and *trans*-$[Mo(phen)(CO)_2\{P(N^tBuCH_2CH_2O)(OMe)\}\{P(N^tBuCH_2CH_2O)\}](OTf)$,[7a] as judged from their relevant bond distances. Therefore, it can be said that the extent of electron donation from amino substituent(s) to phosphenium P depends crucially on the electron donicity of the transition metal fragment. It should be noted that the OMe group in the diaminophosphite ligand(s) in both **1b** and **2b** has no interaction with the neighboring phosphenium P. With **1b**, there seems to be a weak interaction between the phosphenium P and one oxygen of $CF_3SO_3^-$ in the solid state, because the P2···O7 distance is 3.00 Å, which is slightly shorter than the sum of the van der Waals radii of O and P (3.32 Å). A similar weak interaction is indicated for **2b** in the solid state, because the distance between P3 and O6 in $CF_3SO_3^-$ is as short as 3.34 Å.

Complex **4** has a $P(NMeCH_2)_2$ ligand like **1b** and **2b**, but it is electrically neutral, not cationic. This type of complex is generally called a 3e-donor phosphide complex, but it can be considered as a phosphenium complex if one considers it to consist of L_nM^- and $^+P(NMeCH_2)_2$. The Mo(1)−P(2) distance (2.2011(4) Å) is the shortest among the complexes treated in this paper. The geometry around P2 is planar (sum of angles around P2 is 359.94°), but the OMe group in the $P(NMeCH_2)_2(OMe)$ ligand is directed toward the phosphenium P. The P2···O2 distance is 3.25 Å, indicating a weak interaction between phosphenium P and oxygen in the $P(NMeCH_2)_2(OMe)$ ligand, but the OMe is not situated in the middle of the two phosphorus atoms.

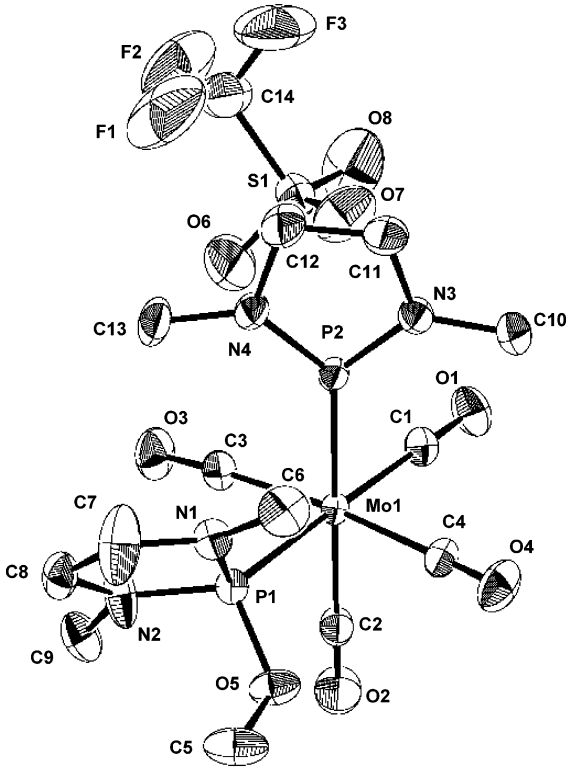

Figure 5. Structure drawing of **1b** with 50% probability ellipsoids. Hydrogen atoms have been omitted.

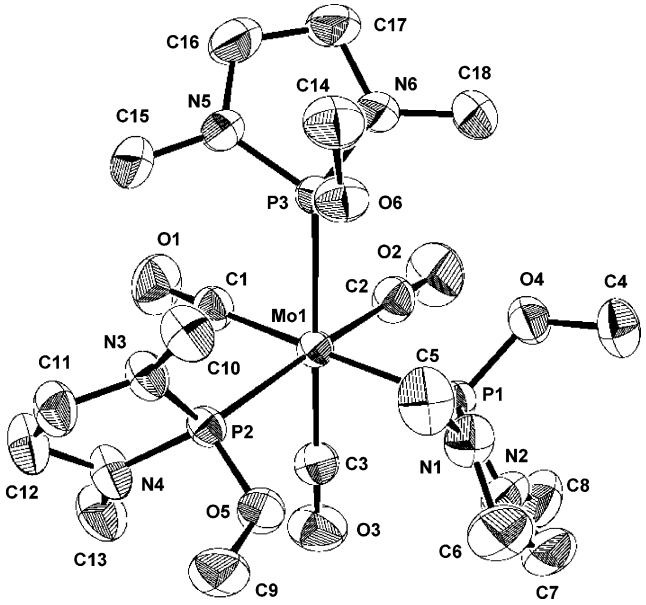

Figure 6. Structure drawing of **2a** with 50% probability ellipsoids. Hydrogen atoms have been omitted.

DFT Calculations for 1b, 4, and 5. The three molybdenum complexes bearing phosphenium and phosphite ligands (**1b**, **2b**, **4**) were prepared and demonstrated to take nonbridging forms exclusively in spite of another possibility to take mirror symmetric bridging forms. In order to gain a clue why a phosphenium phosphite complex prefers a nonbridging form and a silylene alkoxysilyl complex prefers a bridging form, we conducted DFT calculations for cationic and neutral phosphenium phosphite complexes (**1b** and **4**) and a silylene alkoxysilyl complex, $CpMo(CO)_2\{(SiMe_2)_2(OMe)\}$ (**5**). DFT geometry optimization of both bridging and nonbridging forms of these three complexes was successful. The optimized

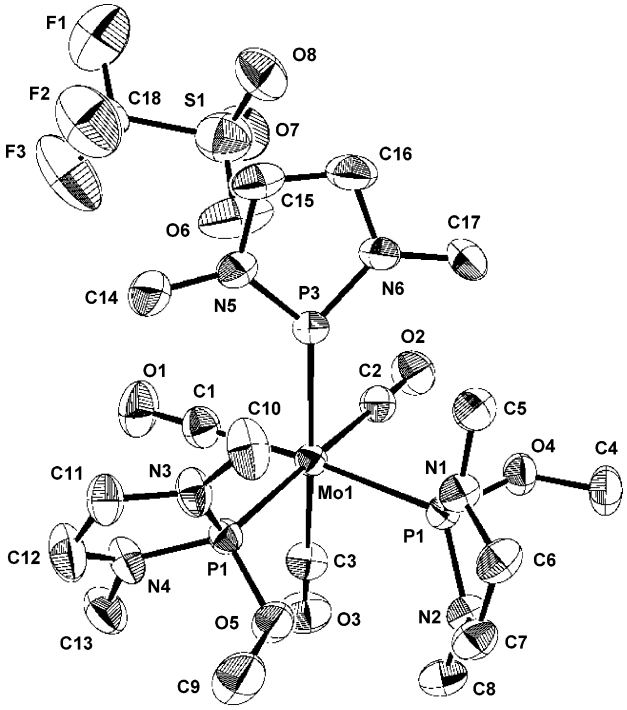

Figure 7. Structure drawing of **2b** with 50% probability ellipsoids. Hydrogen atoms have been omitted.

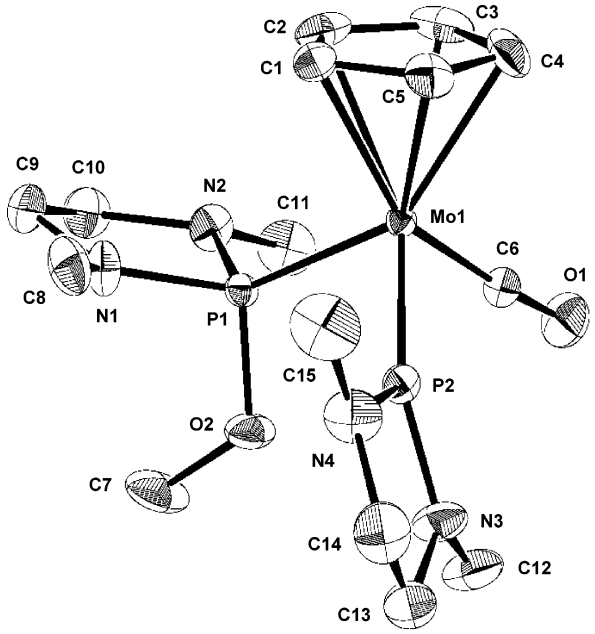

Figure 8. Structure drawing of **4** with 50% probability ellipsoids. Hydrogen atoms have been omitted.

geometries are shown in Figures 9 to 11. Selected bond distances and angles are summarized in Tables 3 to 5.

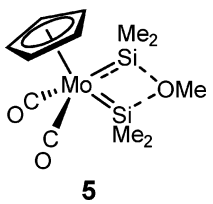

5

For **1b** and **4**, vibrational frequency calculations revealed that only the nonbridging structure was a local minimum (LM) and the bridging structure was a transition state (TS) connecting

Table 1. Summary of Crystal Data for 1b, 2b, 4, and 2a

	1b	2b	4	2a
formula	$C_{14}H_{23}F_3MoN_4O_8P_2S$	$C_{21}H_{43}F_3MoN_6O_8P_3S$	$C_{15}H_{28}MoN_4O_2P_2$	$C_{18}H_{39}MoN_6O_6P_3$
fw	622.30	785.52	454.29	624.40
cryst dimens, mm	0.45 × 0.40 × 0.32	0.50 × 0.18 × 0.35	0.33 × 0.30 × 0.30	0.48 × 0.40 × 0.40
cryst syst	monoclinic	monoclinic	triclinic	monoclinic
space group	$P2_1/c$	$P2_1/c$	$P\bar{1}$	$P2_1/n$
unit cell dimens				
a, Å	10.1270(1)	8.8070 (1)	8.5030(2)	16.703(3)
b, Å	15.7150(3)	21.7500(3)	8.5750(2)	17.963(3)
c, Å	15.5760(4)	17.9600(3)	14.5840(3)	9.744(2)
α, deg	90	90	100.182(1)	90
β, deg	98.7690(1)	99.619(1)	93.405(1)	98.694(16)
γ, deg	90	90	110.024(2)	90
V, Å^3	2449.88(8)	391.91(8)	9754.05(4)	2890.0(10)
Z	4	4	2	4
D_{calcd}, g cm^{-3}	1.687	1.538	1.547	1.435
F(000)	1256.00	1620.00	468	1296
μ, cm^{-1}	8.20	6.569	8.52	6.61
θ range, deg	2.60−27.94	2.97−27.89	3.94−27.94	1.68−30.00
no. of reflns measd	5555	7707	4267	8096
no. of reflns obsd ($I > 2\sigma(I)$)	5369	6788	4239	6714
no. of params	304	376	223	317
R1[a]	0.034	0.058	0.022	0.029
wR2[b]	0.088	0.172	0.061	0.072
GOF	1.058	1.003	1.046	1.025

[a] $R1 = \sum||F_o| - |F_c||/\sum|F_o|$. [b] $wR2 = \{\sum[w(F_o^2 - F_c^2)^2]/\sum[w(F_o^2)^2]\}^{1/2}$; $w = 1/[\sigma^2(F_o^2) + (aP)^2 + bP]$, $P = [2F_c^2 + \mathrm{Max}(F_o^2,0)]/3$.

Table 2. Selected Bond Distances (Å) and Angles (deg) for 1b, 2b, 4, and 2a

1b		2b		4		2a	
Mo(1)−C(1)	2.028(2)	Mo(1)−C(1)	2.000(5)	Mo(1)−P(1)	2.3518(4)	Mo(1)−P(1)	2.5297(6)
Mo(1)−C(2)	2.056(3)	Mo(1)−C(2)	2.013(4)	Mo(1)−P(2)	2.2011(4)	Mo(1)−P(2)	2.5168(6)
Mo(1)−C(3)	2.066(2)	Mo(1)−C(3)	2.029(4)	P(1)−O(2)	1.6387(13)	Mo(1)−P(3)	2.5127(6)
Mo(1)−C(4)	2.044(2)	Mo(1)−P(1)	2.5288(10)	P(1)−N(1)	1.6754(15)	P(1)−O(4)	1.6261(15)
Mo(1)−P(1)	2.4970(6)	Mo(1)−P(2)	2.5116(10)	P(1)−N(2)	1.6878(14)	P(1)−N(1)	1.6701(18)
Mo(1)−P(2)	2.3178(6)	Mo(1)−P(3)	2.3145(10)	P(2)−N(3)	1.6568(17)	P(1)−N(2)	1.6839(18)
P(1)−O(5)	1.6227(19)	P(1)−O(4)	1.622(3)	P(2)−N(4)	1.6723(17)	P(2)−O(5)	1.6285(15)
P(1)−N(1)	1.661(2)	P(1)−N(1)	1.670(4)			P(2)−N(3)	1.6797(17)
P(1)−N(2)	1.652(2)	P(1)−N(2)	1.670(4)			P(2)−N(4)	1.6850(18)
P(2)−N(3)	1.617(2)	P(2)−O(5)	1.612(3)			P(3)−O(6)	1.6293(16)
P(2)−N(4)	1.613(2)	P(2)−N(3)	1.654(4)			P(3)−N(5)	1.6728(17)
O(1)−C(1)	1.136(3)	P(2)−N(4)	1.679(4)			P(3)−N(6)	1.6783(17)
O(2)−C(2)	1.126(3)	P(3)−N(5)	1.620(4)				
O(3)−C(3)	1.126(3)	P(3)−N(6)	1.624(4)				
O(4)−C(4)	1.129(3)						
P(1)−Mo(1)−P(2)	92.19(2)	P(1)−Mo(1)−P(2)	89.56(3)	P(2)−Mo(1)−P(1)	89.749(15)	P(1)−Mo(1)−P(2)	95.29(2)
N(3)−P(2)−Mo(1)	131.40(8)	P(1)−Mo(1)−P(3)	97.24(3)	N(3)−P(2)−N(4)	91.15(9)	P(1)−Mo(1)−P(3)	94.730(19)
N(4)−P(2)−Mo(1)	132.87(8)	P(2)−Mo(1)−P(3)	99.69(4)	N(3)−P(2)−Mo(1)	136.53(6)	P(2)−Mo(1)−P(3)	99.040(19)
N(4)−P(2)−N(3)	95.54(11)	N(5)−P(3)−Mo(1)	132.69(15)	N(4)−P(2)−Mo(1)	132.26(7)	O(4)−P(1)−Mo(1)	106.90(6)
C(10)−N(3)−C(11)	118.4(2)	N(6)−P(3)−Mo(1)	131.94(15)	C(12)−N(3)−C(13)	117.15(18)	N(1)−P(1)−Mo(1)	130.00(7)
C(10)−N(3)−P(2)	127.04(18)	N(6)−P(3)−N(5)	94.3(2)	C(12)−N(3)−P(2)	124.49(13)	N(2)−P(1)−Mo(1)	115.49(7)
C(11)−N(3)−P(2)	114.51(17)	C(14)−N(5)−C(15)	117.5(4)	C(13)−N(3)−P(2)	116.52(15)	O(5)−P(2)−Mo(1)	106.63(6)
C(13)−N(4)−C(12)	119.3(2)	C(14)−N(5)−P(3)	126.1(3)	C(15)−N(4)−C(14)	118.07(19)	N(3)−P(2)−Mo(1)	125.28(6)
C(13)−N(4)−P(2)	124.93(19)	C(15)−N(5)−P(3)	115.6(3)	C(15)−N(4)−P(2)	122.49(16)	N(4)−P(2)−Mo(1)	119.99(7)
C(12)−N(4)−P(2)	114.09(18)	C(16)−N(6)−C(17)	116.7(4)	C(14)−N(4)−P(2)	115.52(16)	O(6)−P(3)−Mo(1)	111.57(6)
		C(16)−N(6)−P(3)	116.2(3)			N(5)−P(3)−Mo(1)	119.77(7)
		C(17)−N(6)−P(3)	127.2(3)			N(6)−P(3)−Mo(1)	119.68(7)

the two nonbridging forms, each of which corresponds to a mirror image. The energy difference between the energy minimum in a nonbridging form and the TS in a bridging form was estimated to be 10.1 kcal/mol for **1b** and 23.5 kcal/mol for **4**. For silylene alkoxysilyl complex **5**, in contrast, both bridging and nonbridging forms were found to have minima. The energy minimum in a bridging form was lower by 21.1 kcal/mol than that in a nonbridging form. The DFT-optimized geometries of the nonbridging structures shown in Figures 9a and 10a agree well with the X-ray structures in Figures 5 and 8. The bridging structure of **5** shown in Figure 11b is also fairly similar to the X-ray structure reported by Ueno et al.[10] Geometric parameters of **1b**, **4**, and **5** listed in Tables 3 to 5 are in good agreement with those obtained by the X-ray analysis, although the calculated values were slightly overestimated.

Comparison of the bond distances and angles in the E−Mo−E−OMe (E = P, Si) portion of the nonbridging form with those of the bridging form has been done to elucidate why a nonbridging form is favorable for phosphenium phosphite complexes, whereas a bridging form is favorable for silylene alkoxysilyl complexes. The P−O bond distance elongates on going from the nonbridging to the bridging forms from 1.645 to 1.939 Å, by 0.294 Å, for **1b** and from 1.668 to 2.048 Å, by 0.380 Å, for **4**. The Si−O distance in **5** elongates from 1.698 to 1.854 Å, only by 0.156 Å. The lengthening is about a half of that for **1b** and **4**. The P−Mo−P angle decreases on going from the nonbridging to the bridging forms from 98.2° to 75.6°, by

(10) Ueno, K.; Masuko, A.; Ogino, H. *Organometallics* **1999**, *18*, 2694.

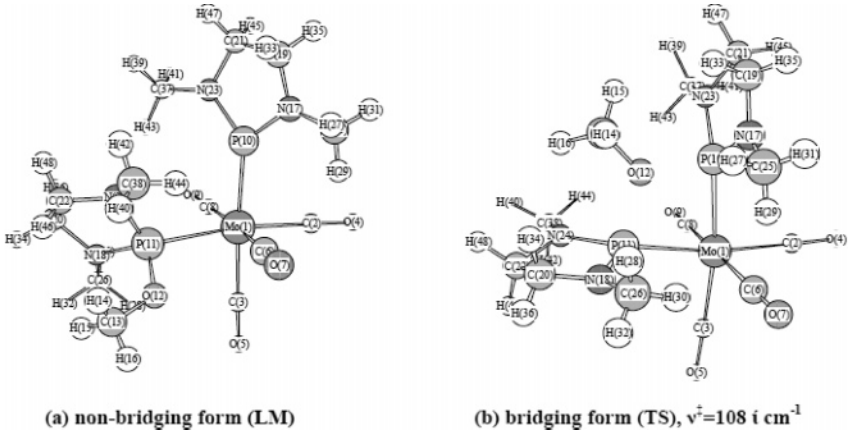

Figure 9. Optimized structures of a nonbridging form (a) and a bridging form (b) of complex **1b** at the B3LYP/SBK(d) level, which were found to be a local minimum (LM) and a transition state (TS), respectively. $\nu^{\ddagger}$ stands for the sole imaginary frequency, which verifies that the obtained geometry is correctly at a saddle point.

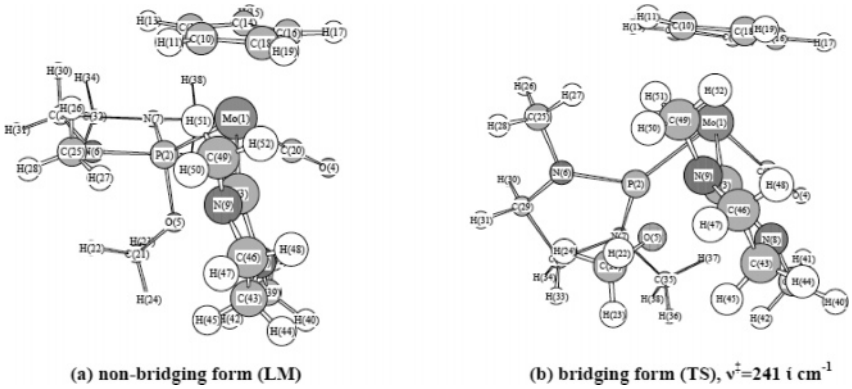

Figure 10. Optimized structures of a nonbridging form (a) and a bridging form (b) of complex **4** at the B3LYP/SBK(d) level, which were found to be a local minimum (LM) and a transition state (TS), respectively. $\nu^{\ddagger}$ stands for the sole imaginary frequency, which verifies that the obtained geometry is correctly at a saddle point.

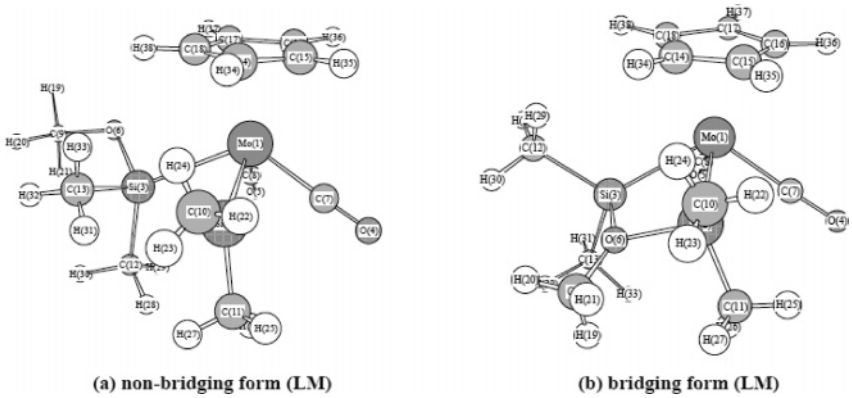

Figure 11. Optimized structures of a nonbridging form (a) and a bridging form (b) of complex **5** at the B3LYP/SBK(d) level, which were found to be local minima (LM).

22.6°, for **1b** and from 95.4° to 78.5°, by 16.9°, for **4**. The Si−Mo−Si angle in **5** also decreases from 71.7° to 64.9°, but only by 6.8°. These changes mean that the cyclization forming the bridge requires larger geometrical changes for phosphenium phosphite complexes than for silylene alkoxysilyl complexes, which is probably responsible for the bridging form being a TS for the phosphenium phosphite complex. With a bridging form, the Si−Mo−Si angle in **5** (64.9°) is considerably smaller than the P−Mo−P angles in **1b** (75.6°) and **4** (78.5°). The smaller angle of **5** may be attributed to its four-legged piano stool geometry, but silylene alkoxysilyl complexes with three-legged piano stool geometries also have relatively small Si−Mo−Si angles (72.6° for Cp*(CO)Fe(SiMe$_2$){SiMe(OMe)}-(OMe) and 70.7° for Cp(CO)Ru{SiMe$_2$}$_2$(OMe)). Therefore, we can say that a silylene alkoxysilyl complex has flexibility in terms of the Si−Mo−Si angle, which renders a bridging form an energy minimum for the silylene alkoxysilyl complex.

Concluding Remarks

Transition metal complexes bearing phosphenium and phosphite ligands in a *cis* position reported to date have carbonyl and bpy (or phen) ancillary ligands. In these complexes, an OR group on the phosphite has no interaction with the phosphenium P, resulting in a nonbridging form. This is in contrast with silylene alkoxysilyl complexes in which the OR group on the

Table 3. Selected Geometric Parameters of 1b at the B3LYP/SBK(d) Level

		nonbridging form	bridging form	expt (X-ray)
bond distance (Å)	Mo(1)−P(10)	2.351	2.486	2.318(1)
	Mo(1)−P(11)	2.569	2.486	2.497(1)
	P(10)−O(12)		1.939	
	P(11)−O(12)	1.645	1.939	1.623(2)
	P(10)−N(17)	1.660	1.671	1.617(2)
	P(10)−N(23)	1.661	1.680	1.613(2)
	P(11)−N(18)	1.697	1.671	1.652(2)
	P(11)−N(24)	1.709	1.680	1.661(2)
	O(12)−C(13)	1.454	1.459	1.444(3)
bond angle (deg)	P(10)−Mo(1)−P(11)	98.2	75.6	92.19(2)
	Mo(1)−P(10)−N(17)	131.6	129.4	131.40(8)
	Mo(1)−P(11)−N(18)	124.0	129.4	119.97(8)
	C(2)−Mo(1)−C(3)	86.8	93.4	91.02(10)
	C(6)−Mo(1)−C(8)	176.5	166.7	174.28(10)
	P(11)−Mo(1)−C(6)	87.0	95.5	86.36(7)
	P(10)−Mo(1)−C(6)	92.6	95.5	90.97(7)
dihedral angle (deg)	Mo(1)−P(10)−N(17)−C(19)	−179.7	166.8	−176.66(17)
	Mo(1)−P(11)−N(18)−C(20)	−124.0	−166.8	−135.6(2)
	C(6)−Mo(1)−P(10)−N(17)	46.5	16.4	34.83(13)
	C(6)−Mo(1)−P(11)−N(18)	−157.9	−16.4	−169.89(14)

Table 4. Selected Geometric Parameters of 4 at the B3LYP/SBK(d) Level

		nonbridging form	bridging form	expt (X-ray)
bond distance (Å)	Mo(1)−P(2)	2.393	2.293	2.352(1)
	Mo(1)−P(3)	2.232	2.293	2.201(1)
	Mo(1)−C(20)	1.950	1.950	1.926(2)
	P(2)−O(5)	1.668	2.048	1.639(2)
	P(3)−O(5)		2.048	
	P(2)−N(6)	1.739	1.713	1.675(2)
	P(2)−N(7)	1.723	1.711	1.688(2)
	P(3)−N(8)	1.708	1.711	1.657(2)
	P(3)−N(9)	1.726	1.713	1.672(2)
	O(5)−C(21)	1.439	1.433	1.434(2)
bond angle (deg)	P(2)−Mo(1)−P(3)	95.4	78.5	89.75(2)
	Mo(1)−P(2)−N(6)	123.6	130.2	121.05(6)
	Mo(1)−P(3)−N(9)	133.0	130.2	132.26(7)
	P(2)−Mo(1)−C(20)	87.9	92.7	87.63(5)
	P(3)−Mo(1)−C(20)	91.0	92.7	91.95(5)
dihedral angle (deg)	Mo(1)−P(2)−N(6)−C(29)	114.2	152.2	123.74(14)
	Mo(1)−P(3)−N(9)−C(46)	−161.7	−152.1	−172.70(13)
	C(20)−Mo(1)−P(2)−N(6)	172.9	−165.1	179.64(9)
	C(20)−Mo(1)−P(3)−N(9)	155.3	165.2	169.80(11)

Table 5. Selected Geometric Parameters of 5 at the B3LYP/SBK(d) Level

		nonbridging form	bridging form	expt (X-ray)[10]
bond distance (Å)	Mo(1)−Si(2)	2.377	2.511	2.4804(9)
	Mo(1)−Si(3)	2.650	2.511	2.4795(9)
	Si(2)−O(6)		1.854	1.782(2)
	Si(3)−O(6)	1.698	1.854	1.788(3)
bond angle (deg)	Si(2)−Mo(1)−Si(3)	71.7	64.9	63.63(3)
	C(7)−Mo(1)−C(8)	78.3	80.7	79.04(14)
dihedral angle (deg)	Mo(1)−Si(2)−C(10)−C(11)	−173.6	−146.8	−145.57
	Mo(1)−Si(3)−C(12)−C(13)	−134.8	146.8	145.00

alkoxysilyl has strong interaction with the silylene Si, resulting in a bridging form. With these phosphenium phosphite complexes the phosphenium is *trans* to bpy and the phosphite is *trans* to CO. This unsymmetrical situation may prevent the complex from taking a bridging form. In this paper, molybdenum carbonyl complexes with two or three diamino-substituted phosphites, *cis*-$[Mo(CO)_4\{P(NMeCH_2)_2(OMe)\}_2]$ (**1a**) and *fac*-$[Mo(CO)_3\{P(NMeCH_2)_2(OMe)\}_3]$ (**2a**), were prepared and their reactions with TMSOTf were examined. A single OMe^- abstraction reaction from one of the coordinating phosphite ligands took place to form phosphenium phosphite complexes **1b** and **2b**, with the original configuration around the Mo kept unchanged. The X-ray structure analyses and the NMR spectra showed that these complexes have no interaction between the OMe group in the phosphite ligand and the phosphenium P. $CpMo(CO)(I)\{P(NMeCH_2)_2(OMe)\}_2$ (**3**) was unexpectedly converted into a neutral phosphenium phosphite complex **4** in the reaction with $NaK_{2.8}$. This complex also has no strong O···P(phosphenium) interaction. If these complexes (**1b**, **2b**, **4**) have a strong O···P(phosphenium) interaction and the OMe is situated at the middle point between the original phosphite P and phosphenium P, then the resulting complexes would have a bridging form with mirror symmetry.

DFT calculations were performed for phosphenium phosphite complexes (**1b** and **4**) and a silylene alkoxysilyl complex (**5**). For **1b** and **4** a nonbridging form is a local minimum and a bridging form is a transition state with an energy difference of 10.1 kcal/mol for **1b** and 23.5 kcal/mol for **4**. In contrast, for silylene alkoxysilyl complex **5**, both nonbridging and bridging forms are minima and the bridging form is more stable by 21.2 kcal/mol than the nonbridging form. Comparison of structural features revealed that the bridging requires large geometrical changes for phosphenium phosphite complexes than for silylene alkoxysilyl complexes.

Experimental Section

General Remarks. All reactions were carried out under an atmosphere of dry nitrogen by using Schlenk tube techniques. CH_2Cl_2 was distilled from P_2O_5, and hexane and THF were distilled from sodium metal. These were stored under nitrogen atmosphere. $P(NMeCH_2)_2(OMe)$,[11] $Mo(CO)_4(nbd)$,[12] $Mo(CO)_3(NCMe)_3$,[13] and $CpMo(CO)_3I$[14] were prepared according to the literature methods.

Photoirradiation was performed with a 400 W medium-pressure mercury arc lamp at 0 °C. IR spectra were recorded on a Perkin-Elmer Spectrum One spectrometer. A JEOL LA-300 multinuclear spectrometer and JEOL JNM-AL400 spectrometer were used to obtain ^1H, ^{13}C, and ^{31}P NMR spectra. ^1H and ^{13}C NMR data were referenced to Me_4Si. ^{31}P NMR data were referenced to 85% H_3PO_4.

Preparation of *cis*-[Mo(CO)$_4${P(NMeCH$_2$)$_2$(OMe)}$_2$] (1a). A CH_2Cl_2 solution (15 mL) containing $Mo(CO)_4(nbd)$ (1.50 g, 5.00 mmol) and $P(NMeCH_2)_2(OMe)$ (1.8 mL, 12.9 mmol) was stirred for 30 min at room temperature. Volatile materials were removed under reduced pressure. The resulting white solid was washed with 5 mL of hexane three times at −30 °C, collected by filtration, and dried in vacuo to give a white powder of **1a** (2.10 g, 4.16 mmol, 83%). Anal. Calcd for $C_{14}H_{26}N_4O_6P_2Mo$: C, 33.35; H, 5.20; N, 11.11. Found: C, 33.02; H, 5.10; N, 11.06. ^1H NMR (δ, in $CDCl_3$): 2.77 (fd, J_{PH} = 11.19 Hz, 12H, NCH_3), 3.16 (m, 4H, NCH_2), 3.20 (fd, J_{PH} = 13.19 Hz, 6H, OCH_3), 3.29 (m, 4H, NCH_2). $^{13}C\{^1H\}$ NMR (δ, in $CDCl_3$): 33.21 (m, NCH_3), 50.58 (m, OCH_3), 50.89 (s, NCH_2), 209.90 (t, J_{PC} = 12.1 Hz, CO), 214.52 (t, J_{PC} = 12.1 Hz, CO). $^{31}P\{^1H\}$ NMR (δ, in $CDCl_3$): 147.4 (s). IR (cm^{-1}, in CH_2Cl_2): ν(CO) 2026, 1929, 1914.

Preparation of *cis*-[Mo(CO)$_4${P(NMeCH$_2$)$_2$(OMe)}{P(NMeCH$_2$)$_2$}]OTf (1b). A solution of **1a** (0.43 g, 0.84 mmol) in CH_2Cl_2 (10 mL) was cooled at −78 °C, and TMSOTf (0.15 mL, 0.84 mmol) was added dropwise. The solution was allowed to warm gradually to room temperature and stirred for 1 h. Allowing the solution to stand at −30 °C for 1 day led to the formation of yellow crystals, which were isolated by filtration and dried in vacuo to give **1b**. ^1H NMR (δ, in $CDCl_3$ at −60 °C): 2.71 (fd, J_{PH} = 11.19 Hz, 6H, NCH_3), 2.80 (d, J_{PH} = 10.39 Hz, 3H, NCH_3), 3.07 (d, J_{PH} = 9.19 Hz, 3H, NCH_3), 3.07 (m, 2H, NCH_2), 3.20 (m, 2H, NCH_2), 3.23 (d, J_{PH} = 10.39 Hz, 3H, OCH_3), 3.91 (m, 4H, NCH_2). $^{13}C\{^1H\}$ NMR (δ, in $CDCl_3$ at −60 °C): 32.78 (d, J_{PC} = 12.4 Hz, NCH_3), 33.62 (m, NCH_3), 50.09 (d, J_{PC} = 9.1 HZ, OCH_3), 51.04 (m, NCH_2), 51.77 (m, NCH_2), 52.40 (m, NCH_2), 203.01 (t, J_{PC} = 12.4 Hz, CO), 206.07 (m, CO). $^{31}P\{^1H\}$ NMR (δ, in $CDCl_3$, at −60 °C): 138.47 (d, J_{PP} = 41.7 Hz, $P(NMeCH_2)_2(OMe)$), 286.57 (d, J_{PP} = 41.7 Hz, $P(NMeCH_2)_2$). IR (cm^{-1}, in CH_2Cl_2): ν(CO) 2042, 1934.

Preparation of *fac*-[Mo(CO)$_3${P(NMeCH$_2$)$_2$(OMe)}$_3$] (2a). A THF solution (20 mL) containing $Mo(CO)_3(NCMe)_3$ (0.44 g, 1.50 mmol) and $P(NMeCH_2)_2(OMe)$ (0.68 mL, 4.7 mmol) was stirred for 4 h at room temperature. A precipitate formed, which was collected by filtration, washed with hexane a few times, and dried in vacuo to give a white powder of **2a** (0.66 g, 1.10 mmol, 71%). Anal. Calcd for $C_{18}H_{39}N_6O_6P_3Mo$: C, 34.62; H, 6.30; N, 13.46. Found: C, 34.47; H, 6.26; N, 13.33. ^1H NMR (δ, in $CDCl_3$): 2.80 (m, 18H, NCH_3), 3.14 (m, 6H, NCH_2), 3.17 (m, 9H, OCH_3), 3.27 (m, 6H, NCH_2). $^{13}C\{^1H\}$ NMR (δ, in $CDCl_3$): 33.59 (m, NCH_3), 50.20 (m, OCH_3), 52.25 (m, NCH_2), 218.28 (m, CO). $^{31}P\{^1H\}$ NMR (δ, in $CDCl_3$): 149.36 (s). IR (cm^{-1}, in cyclohexane): ν(CO) 1841, 1944.

Preparation of *fac*-[Mo(CO)$_3${P(NMeCH$_2$)$_2$(OMe)}$_2${P(NMeCH$_2$)$_2$}]OTf (2b). A solution of **2a** (0.80 g, 1.28 mmol) in CH_2Cl_2 (5 mL) was cooled at −78 °C, and TMSOTf (0.23 mL, 1.28 mmol) was added dropwise. The solution was allowed to warm gradually to room temperature and stirred for 1 h. Addition of hexane (20 mL) to the solution yielded a yellow precipitate, which was collected by filtration, washed with hexane, and dried in vacuo to give **2b**. ^1H NMR (δ, in $CDCl_3$ at −60 °C): 2.56 (fd, J_{PH} = 10.79 Hz, 6H, NCH_3), 2.67 (fd, J_{PH} = 11.19 Hz, 6H, NCH_3), 2.99 (m, 2H, NCH_2), 3.04 (fd, J_{PH} = 10.79 Hz, 6H, NCH_3), 3.10 (m, 2H, NCH_2), 3.20 (fd, J_{PH} = 9.99 Hz, 6H, OCH_3), 3.30 (m, 4H, NCH_2) 3.84 (m, 4H, NCH_2). $^{13}C\{^1H\}$ NMR (δ, in $CDCl_3$ at −60 °C): 32.75 (m, NCH_3), 32.98 (m, NCH_3), 33.90 (m, NCH_3), 50.52 (m, NCH_2), 51.59 (m, NCH_2), 52.05 (m, OCH_3), 52.30 (m, OCH_3), 210.47 (m, CO). $^{31}P\{^1H\}$ NMR (δ, in $CDCl_3$ at −60 °C): 141.84 (d, J_{PP} = 41.7 Hz, $P(NMeCH_2)_2(OMe)$), 275.74 (t, J_{PP} = 41.6 Hz, $P(NMeCH_2)_2$). IR (cm^{-1}, in CH_2Cl_2): ν(CO) 2017, 1959, 1917.

Preparation of CpMo(CO)I{P(NMeCH$_2$)$_2$(OMe)}$_2$ (3). $P(NMeCH_2)_2(OMe)$ (0.68 mL, 4.7 mmol) was added to a solution of $CpMo(CO)_3I$ (0.83 g, 2.23 mmol) in THF (20 mL) at 0 °C. After photoreaction of the solution for 16 h, a precipitate formed, which was collected by filtration, washed with hexane a few times, and dried in vacuo to give a red powder of **3** (1.22 g, 1.99 mmol, 89%). Anal. Calcd for $C_{16}H_{31}IN_4O_3P_2Mo$: C, 31.39; H, 5.10; N, 9.15. Found: C, 31.12; H, 5.01; N, 8.92. ^1H NMR (δ, in $CDCl_3$): 2.69 (fd, J_{PH} = 10.52 Hz, 6H, NCH_3), 2.90 (fd, J_{PH} = 10.61 Hz, 6H, NCH_3), 3.18 (m, 4H, NCH_2), 3.32 (m, 4H, NCH_2), 3.34 (fd, J_{PH} = 10.61 Hz, 6H, OCH_3), 5.16 (s, 5H, C_5H_5). $^{13}C\{^1H\}$ NMR (δ, in $CDCl_3$): 34.61 (m, NCH_3), 51.74 (m, OCH_3), 52.80 (s, NCH_2), 54.04 (s, NCH_2), 89.01 (s, C_5H_5), 265.74 (t, J_{PC} = 36.0 Hz, CO). $^{31}P\{^1H\}$ NMR (δ, in $CDCl_3$): 159.22 (s). IR (cm^{-1}, in CH_2Cl_2): ν(CO) 1805.

Preparation of CpMo(CO){P(NMeCH$_2$)$_2$(OMe)}{P(NMeCH$_2$)$_2$} (4). $NaK_{2.8}$ (0.14 mL, 0.90 mmol) was added to a solution of **3** (0.22 g, 0.36 mmol) in THF (20 mL). After being stirred for 3 h at room temperature, the solution was filtered and the filtrate was dried under reduced pressure. Hexane (20 mL) was added to the residue, and the solution was filtered to remove undissolved materials. The solvent was removed under reduced pressure, and the resulting yellow powder was washed with cold hexane (5 mL) and dried to give **4** (0.05 g, 0.011 mmol, 31%). Anal. Calcd for $C_{15}H_{28}IN_4O_2P_2Mo$: C, 39.66; H, 6.21; N, 12.33. Found: C, 39.45; H, 6.19; N, 12.05. ^1H NMR (δ, in $CDCl_3$): 2.65 (d, J_{PH} = 11.45 Hz, 3H, NCH_3), 2.71 (d, J_{PH} = 11.42 Hz, 3H, NCH_3), 2.78 (d, J_{PH} = 10.83 Hz, 6H, NCH_3), 2.73 (m, 4H, NCH_2), 2.98 (m, 4H, NCH_2), 3.15 (d, J_{PH} = 10.80 Hz, 3H, OCH_3), 5.28 (s, 5H, C_5H_5). $^{13}C\{^1H\}$ NMR (δ, in $CDCl_3$): 34.31 (d, J_{PC} = 17.2 Hz, NCH_3), 34.63 (d, J_{PC} = 13.2 Hz, NCH_3), 34.74 (d, J_{PC} = 13.2 Hz, NCH_3), 50.70, d, J_{PC} = 11.4 Hz, OCH_3), 51.22 (d, J_{PC} = 4.5 Hz, NCH_2), 51.53 (d, J_{PC} = 5.3 Hz, NCH_2), 51.80 (d, J_{PC} = 3.8 Hz, NCH_2), 85.90 (s, C_5H_5), 240.71 (t, J_{PC} = 20.0 Hz, CO). $^{31}P\{^1H\}$ NMR (δ, in $CDCl_3$): 194.74 (d, J_{PP} = 61.2 Hz, $P(NMeCH_2)_2(OMe)$), 250.44 (d, J_{PP} = 61.2 Hz, $P(NMeCH_2)_2$).

Crystallographic Study. Suitable crystals of **1b**, **2a**, **2b**, and **4** were mounted separately on a glass fiber. All measurements for **1b**, **2b**, and **4** were made on a Mac Science DIP2030 imaging plate area detector, while those for **2a** were made on a Mac Science MXC3κ. The data were collected to a maximum 2θ value of 55°. Cell parameters and intensities for the reflection were estimated using the program packages of HKL for **1b**, **2b**, and **4** and MXC-system for **2a**.[15,16] The structures were solved by direct methods and expanded using Fourier techniques. Non-hydrogen atoms were refined anisotropically. Hydrogen atoms were located at ideal positions and refined isotropically. In the crystal of **2b**, a hexane

(11) Ramirez, F.; Patwardham, A. V.; Kugler, H. J.; Smith, C. P. *J. Am. Chem. Soc.* **1967**, *89*, 6276.
(12) Bennett, M. A.; Pratt, L.; Wilkinson, G. *J. Chem. Soc.* **1961**, 2037.
(13) Tape, D. P.; Knipple, W. R.; Augl, J. M. *Inorg. Chem.* **1962**, *1*, 433.
(14) Wrighton, M. S.; Ginley, D. S. *J. Am. Chem. Soc.* **1975**, *97*, 4246.
(15) Otwinowski, Z.; Minor, W. In *Processing of X-ray Diffraction Data Collected in Oscillation Mode, Methods in Enzymology*, Vol. 276: *Macromolecular Crystallography*, Part A; Carter, C. W., Jr., Sweet, R. M., Eds.; Academic Press: New York, 1997; pp 307−326.
(16) *MXC-system*; A program system for data collection and reduction; Mac Science Co. Ltd.: Yokohama, Japan, 1995.

molecule was found to occupy a space around the crystallographic inversion center, and half the molecule, C_3H_7, was refined as a rigid group. All calculations were performed using the SHELXL-97 crystallographic software package.[17]

DFT Calculations. Geometry optimizations of both nonbridging and bridging forms of phosphenium complexes **1b** and **4** were carried out using the hybrid B3LYP functional approach of the density functional theory with the effective core potential (ECP) proposed by Stevens et al.,[18] SBK, with double-ζ plus polarization functions, which was denoted as SBK(d) in this paper. B3LYP was assembled with Becke's three-parameter exchange functional[19] and the Lee−Yang−Parr correlation gradient−corrected functional.[20] Geometry searches for the two forms of silylene complex **5** were also performed for comparison. Vibrational analysis based on force constant matrices (Hessians) at the B3LYP/SBK(d) level was carried out at the stationary points in order to identify them as minima (all positive constants), transition states (one negative force constant), or higher-order saddle points. The Gaussian 98 program package[21] was used for all calculations. The computers used in this study are Linux PC cluster machines at Ochanomizu University and the computer facilities at the Research Center for Computational Science in Okazaki, Japan.

Acknowledgment. This work was supported by a Grant-in Aid (No. 15205010) and by a Grant-in-Aid for Science Research on Priority Area (No. 18033044, Chemistry of Coordination Space) from the Ministry of Education, Culture, Sports, Science and Technology. The authors thank the Research Center for Computational Science in Okazaki, Japan, for the use of the computer facilities.

Supporting Information Available: X-ray crystallographic data in CIF format for complexes **1b**, **2a**, **2b**, and **4**. This material is available free of charge via the Internet at http://pubs.acs.org.

OM060639X

(17) Scheldrick, G. M. *SHELX-97*, Programs for Crystal Structure Analysis; University of Göttingen: Germany, 1997.

(18) Stevens, W. J.; Krauss, M.; Basch, H.; Jasien, P. G. *Can. J. Chem.* **1992**, *70*, 612.

(19) Becke, A. D. *J. Chem. Phys.* **1993**, *98*, 5648.

(20) Lee, C.; Yang, W.; Parr, R. G. *Phys. Rev. B* **1988**, *37*, 785.

(21) Frisch, M. J.; Trucks, G. W.; Schlegel, H. B.; Scuseria, G. E.; Robb, M. A.; Cheeseman, J. R.; Zakrzewski, V. G.; Montgomery, J. A., Jr.; Stratmann, R. E.; Burant, J. C.; Dapprich, S.; Millam, J. M.; Daniels, A. D.; Kudin, K. N.; Strain, M. C.; Farkas, O.; Tomasi, J.; Barone, V.; Cossi, M.; Cammi, R.; Mennucci, B.; Pomelli, C.; Adamo, C.; Clifford, S.; Ochterski, J.; Petersson, G. A.; Ayala, P. Y.; Cui, Q.; Morokuma, K.; Malick, D. K.; Rabuck, A. D.; Raghavachari, K.; Foresman, J. B.; Cioslowski, J.; Ortiz, J. V.; Baboul, A. G.; Stefanov, B. B.; Liu, G.; Liashenko, A.; Piskorz, P.; Komaromi, I.; Gomperts, R.; Martin, R. L.; Fox, D. J.; Keith, T.; Al-Laham, M. A.; Peng, C. Y.; Nanayakkara, A.; Gonzalez, C.; Challacombe, M.; Gill, P. M. W.; Johnson, B.; Chen, W.; Wong, M. W.; Andres, J. L.; Head-Gordon, M.; Replogle, E. S.; Pople, J. A. *Gaussian 98*; Gaussian, Inc.: Pittsburgh, PA, 1998.